

## FATIGUE CRACK PROPAGATION IN SHEET SPECIMENS

W. Weibull

After having examined a large number of test data on fatigue crack propagation in sheet specimens I felt convinced that the rate of crack propagation  $dl/dN$  is, independently of the crack length  $l$ , determined by the nominal stress amplitude  $\sigma$  computed as the ratio of the load amplitude and the remaining cross-sectional area, and also by some parameters that define the test conditions, such as mean stress  $\sigma_m$ , stress ratio  $R$ , pre-stress history, dimensions of specimen, temperature, frequency and, of course, some relevant properties of the material.

It is an essential assumption that the crack length  $l$  does not explicitly enter into the basic propagation formula as has previously always been assumed, particularly by English scientists (Frost, Dugdale and others) who strongly objected to my assumption and advocated that the rate is proportional to the crack length.

The basic propagation formula can be put in the following form

$$dx/dN = k(\sigma - \sigma_e)^\beta \quad (1)$$

where  $x = l/w =$  relative crack length, that is, the crack length divided by the specimen width,  $N =$  the number of cycles,  $k$  and  $\beta$  constants depending not only on the material but also on the testing conditions, and  $\sigma_e$  a kind of endurance limit, insofar as for  $\sigma \leq \sigma_e$  the crack does not propagate and consequently the fatigue life becomes infinitely large.

#### 1. The Three Types of Repeated Stress Cycles

In the case of complete reversal ( $R = -1$ ) three types of repeated load or stress cycles can be distinguished: (a) constant load amplitude, (b) constant stress amplitude, and (c) decreasing load and stress amplitude.

##### (a) Constant Load Amplitude Tests

The maximum tensile and compressive stresses are based on the original net cross-sectional area. Thus, the load cycle is kept constant throughout the entire test and, consequently, the nominal stress is permitted to increase as demonstrated in Fig. 1a. The fact that during the compressive part of the cycle the fatigue crack closes fully and the cracked portion of the specimen continues to carry load has been verified by use of strain gage and photo-elastic strain measurements. Therefore the maximum compressive stress remains constant.

## (b) Constant Stress Amplitude Tests

The maximum tensile stress is based on the remaining cross-sectional area, while the maximum compressive stress is based on the original net area. Therefore the maximum tensile load has to be reduced periodically throughout the test in proportion to the decreasing area, while the maximum compressive load is maintained constant as demonstrated in Fig. 1b.

## (c) Decreasing Load and Stress Amplitude Tests

Both the maximum tensile and compressive load are reduced periodically throughout the test as demonstrated in Fig. 1c.

In the case of zero-to-tension stress cycles ( $R = 0$ ) only the first two types exist, and I will confine myself to these.

## 2. Constant Stress Amplitude Tests

The basic formula (1) applies, since the nominal stress due to the successive reduction of the load amplitude becomes

$$\sigma = \sigma_i = \text{constant} \quad (2)$$

where  $\sigma_i$  is the stress amplitude by which the crack has been initiated. The form

$$dx/dN = k(\sigma_i - \sigma_e)^\beta = k' = \text{constant} \quad (3)$$

and after integration

$$x = k'(N - N_0) \quad (4)$$

where  $N_0$  is the arbitrarily chosen number of cycles at which the crack propagation starts after a certain initiation period  $N_1$ , or sometimes after a following "transition period."

Some results of an extensive test program, conducted at the Aeronautical Research Institute of Sweden (FFA), Stockholm, are listed.

Fig. 2 shows the result from tests on specimens geometrically similar (except that the thickness of the specimen was kept constant,  $t = 2\text{mm}$ ). The material was an aluminum alloy, 24S-T, and the constant stress amplitude  $\sigma = 12/2 \text{ kg/mm}^2$  ( $R = 0$ ). The crack length in millimeters (mm) is plotted against the number of cycles in kilocycles (kc). The linear relationship between crack length and number of cycles, mathematically expressed by Eq. (4), is most excellently verified.

There is, however, another conclusion that can be drawn from this set of curves and that is, as I have already indicated, that the rate of crack propagation, which is equal to the slope of the straight lines, is proportional to the width of the specimen. (Please note that the width goes from

w = 170.6 mm down to w = 22.7 mm). This observation implies that if the relative length  $x = l/w$  is plotted against the number of cycles, then a set of parallel lines will result. It further implies that the propagation period, for equal stress amplitudes, is independent of the specimen width. This is why I have introduced  $x$  instead of  $l$  in the basic formula (1).

Fig. 3 shows the same result for geometrically similar specimens of 75S-T aluminum alloy ( $\sigma = 12/2 \text{ kg/mm}^2$ ,  $R = 0$ ).

Quite recently a test on a specimen of a titanium alloy has been performed at the FFA with the same result. Furthermore, Eq. (4) has been confirmed by Rolfe and Munse by tests on specimens of aged and unaged mild steel with widths of 5 and 7 in. at completely reversed stress cycles of different amplitudes, and at the temperatures  $78^\circ\text{F}$  and  $-40^\circ\text{F}$ . Also Massonet, Belgium, and associates have studied the rate of propagation in mild steel specimens subjected to repeated bending. Since the result was the same, it therefore seems safe to say that this law has been verified.

Fig. 4 describes the so-called transition period, which in some cases precedes the linear stage of propagation. The codes of the two series mean: stress amplitude/width of specimen/width of central aperture/thickness of specimen,

and the appendix x notched by circular hole and sl a central slit.

The main difference between the two specimens is in the central apertures. In the left-hand curve the very short initiation period is due to the large aperture (12 o/o), while in the right-hand curve the long initiation period of some 30,000 cycles is caused by the small aperture (2 o/o). (It has been proved theoretically and experimentally that there is a considerable statistical size effect on the duration of the initiation period.) In the first case, the linear stage (constant rate) starts almost immediately, whereas in the second case there is a transition period of about 200 kc before the linear stage sets in. During the transition period the rate of propagation is gradually increasing until the constant value is reached. This part of the curve can be mathematically represented by the formula

$$dl/dN = k \cdot l \cdot \sigma^m \quad (5)$$

as proposed by Frost and Dugdale and others, that is, the rate appears to be proportional to the crack length. I refuse to accept this geometrical interpretation of the first part of the curve due to the fact that the transition period essentially depends on the stress pre-history. If there is a long initiation period, then there always follows a long transition period, and if there is a very short initiation

period, then there may be in a specimen of the same shape no transition period at all. If the specimen in the left-hand test had been subjected to a high static pre-load prior to the fatigue test, a transition period quite as long as that in the right-hand test would have been generated. My interpretation therefore is that during the initiation of the crack, residual stresses are built up in the vicinity of the crack tip, and this part of the specimen has to be passed before the linear stage sets in. I will presently give some more evidence of this interpretation in connection with two-level crack propagation tests.

### 3. Constant Load Amplitude Tests

Since in this case the nominal stress amplitude  $\sigma$  increases with the relative crack length  $x$  as

$$\sigma = \sigma_o / (1 - x) \quad (6)$$

where  $\sigma_o$  is the nominal gross stress amplitude, that is,  $\sigma_o = L/w \cdot t$ , thus the initiating stress amplitude is

$$\sigma_i = \sigma_o / (1 - x_i) \quad (7)$$

where  $x_i$  is the relative width of the central aperture.

Introducing (6) into (1) we have

$$dx/dN = k(\sigma_o / (1-x) - \sigma_e)^\beta = k[(\sigma_o - \sigma_e + \sigma_e \cdot x) / (1-x)]^\beta \quad (8)$$

or

$$dx/dN = k(\sigma_o - \sigma_e)^\beta [(1+c \cdot x)/(1-x)]^\beta \quad (9)$$

where

$$c = \sigma_e / (\sigma_o - \sigma_e) \quad (10)$$

This basic formula involves three parameters:  $k$ ,  $\beta$ , and  $\sigma_e$  or  $k$ ,  $\beta$ , and  $c$ , since  $\sigma_e$  and  $c$  are linked by Eq. (10).

By integration we have

$$\int_0^x [(1-x)/(1+c \cdot x)]^\beta dx = k(\sigma_o - \sigma_e)^\beta (N - N_o) \quad (11)$$

Putting

$$Y_o^x = \int_0^x [(1-x)/(1+c \cdot x)]^\beta dx \text{ and } Y_o^1 = \int_0^1 [(1-x)/(1+c \cdot x)]^\beta dx \quad (12)$$

and

$$y = Y_o^x / Y_o^1 \quad (13)$$

we have

$$y = k''(N - N_o) \quad (14)$$

where

$$k'' = k(\sigma_o - \sigma_e)^\beta / Y_o^1 = \text{constant} \quad (15)$$

It should be noted that  $y$  is a function of the relative crack length  $x$ , involving the two parameters  $\beta$  and  $c$ , the latter uniquely determined by the constant stress amplitude  $\sigma_o$  and the endurance limit  $\sigma_e$ .



From the definition (13) of  $y$ , it follows that

$$y = 0 \text{ for } x = 0 \text{ and } y = 1 \text{ for } x = 1$$

The quantity  $Y_0^1$  is a constant, uniquely determined by  $\beta$  and  $c$ . For the practical evaluation of test data, the function  $y$  has been computed and tabulated for selected values of  $\beta$  and  $c$ .

From Eq. (14) it follows that if the values of  $y$ , corresponding to the proper values of  $\beta$  and  $\sigma_e$ , are plotted against  $N$  a straight line will result.

From Eqs. (14) and (15) it is readily seen that for a given imposed stress amplitude  $\sigma_0$  the crack propagation, that is, the relationship between  $x$  and  $N$ , is uniquely determined by the three parameters  $k$ ,  $\beta$  and  $\sigma_e$ . A fourth parameter  $N_0$  is also involved, but this quantity can, as the origin of the time scale, be arbitrarily chosen. An extensive program to determine these three parameters under various testing conditions has been carried through at the FFA, Stockholm, and the time-absorbing evaluation work has been sponsored by the Air Force Materials Laboratory, Research and Technology Division, AFSC, through the European Office of Aerospace Research, United States Air Force.

Now, as we have an equation that links  $x$  and  $N$  by means of three parameters, it is theoretically sufficient to

measure three data points  $(x_m, N_m)$   $m = 1, 2, 3$ . Since the measurement of the crack length is not too easy and there is a scatter due to the material, it is safer to use more than three points. The practical procedure therefore consists in plotting  $y$  against  $N$  by choosing the parameters in such a way that a large set of points  $(y_k, N_k)$  plot on a straight line. This procedure has been successfully performed with data from tests under quite different test conditions.

Crack propagation can be represented very easily by means of straight lines (Fig. 5) for each test series on the  $y$  vs.  $N$  scales. (The code numbers are, as usual,  $\sigma_0/w/s/2r$  where  $s$  = width of slit and  $r$  = root radius of slit.)

However, when plotting the complete test from the initiation of the crack until final failure of the specimen, it was immediately observed that the curve was, in most cases, composed of three parts, each plotting as a straight line but with different slopes. This is easily explained by an examination of the fracture surface. It is a well-known fact that there are three different modes of failure that change at certain lengths of the crack, but depend both on the imposed stress amplitude and the dimensions of the specimen.

Since some of the parameters change with the mode of failure, it is important to know what mode of failure you are examining when comparing results from different tests. This obvious necessity has frequently been neglected in earlier discussions and has led to erroneous conclusions. That this is a complicated problem may be demonstrated by means of Fig. 6. For example, for a crack length of 20 o/o the four first diagrams have different modes of failure. Liu's theory predicts the change-over points quite satisfactorily.

Fig. 7 represents the results of three replicated propagation tests, only one of which shows all three stages carried out at the NLR in Amsterdam. The three curves have the same  $\beta$  and  $c$  values, which implies that they can be plotted to the same y-scale. The difference in slope is due to differences in the value of  $k$  and the shift in horizontal direction is due to differences in the duration of the initiation period. The imposed amplitude  $\sigma_o = 5.49 \text{ kg/mm}^2$  and the evaluated value of  $\sigma_e$  is  $\sigma_e = 2.70 \text{ kg/mm}^2$ .

Fig. 8 shows three replicated tests on specimens identical with those in the preceding figure but subjected to a lower stress amplitude,  $\sigma_o = 2.41 \text{ kg/mm}^2$ . Here the scatter of the curves is due mainly to different lengths of the initiation periods, but the exciting thing about these

curves is that the endurance limit now is only  $\sigma_e = 0.22 \text{ kg/mm}^2$  compared to 2.70 at the higher stress level. Other tests have confirmed that  $\sigma_e$  is not a material constant but depends on the imposed load. When presenting this observation at the ICAF-AGARD Symposium in Rome, in April 1963, Dr. P. J. E. Forsyth, RAE, Farnborough, United Kingdom, indicated that he had found, after extensive metallographic work, that the root radius of the crack increased with the imposed load. Since this implies a decrease of the stress concentration factor, his observations comply with my purely phenomenological finding.

These results give a natural explanation of the curves from the two-level tests conducted at the NLR, Netherlands, and reported by Schijve et al. For this reason I have evaluated the data and for this purpose the curves have been replotted by substituting  $N/N_B$  scales for the N-scales. as demonstrated in Fig. 9. Since the value of  $c$  differs for the two stress levels, different y-scales must be used.

The same plotting technique has been applied to two-level tests of NLR. In Fig. 10 the results from a two-level test, started from the high level, are plotted. The first three points use the left-hand scale. At  $x = 7.5$  per cent the lower level is applied and the following six points are

plotted by use of the right-hand scale. At the beginning of this period it may be assumed that  $\sigma_e = 2.70 \text{ kg/mm}^2$  and that this value gradually decreases until it reaches the value  $\sigma_e = 0.22 \text{ kg/mm}^2$ . This conclusion is indicated by the fact that the curve becomes a straight line with practically the same slope as found in the single-level tests. The preceding high load has produced an additional fatigue life of 7 o/o. At  $x = 15.4$  per cent the higher level is applied. The value of  $\sigma_e$  appears to take its higher value almost instantaneously, with a loss in fatigue life of about 2 per cent only. The upper part of the y-scale is very compact, so this part of the diagram is replotted on larger scales in Fig. 11. At  $x = 22.4$  per cent the lower level is applied. The value of  $\sigma_e$  decreases gradually with an increase in fatigue life of 5 per cent and the curve is then remarkably straight until final failure occurs. Computed according to the Palmgren-Miner rule, the total fatigue life is 101 per cent, which is very close, but this coincidence seems to be casual as demonstrated in Fig. 12 by a test which was started from the lower level. This diagram presents the same general aspect as the preceding one with large gains in life when the load is dropped and small losses in life when the load is raised. The upper part of the diagram is replotted on larger scales in Fig. 13.

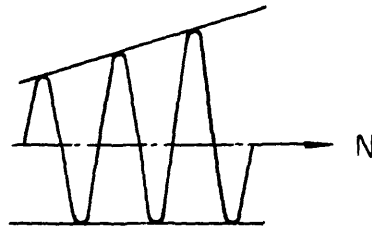
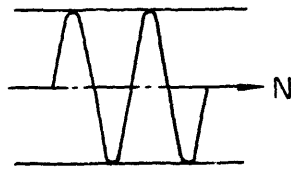
The two diagrams are compared in Fig. 14. Such diagrams can easily be extended to any number of stress levels, provided corresponding single-level tests have been performed. The influence of arbitrary program loadings and of the sequences of the loads will in this way be predictable from appropriate single-level tests.

### List of Figures

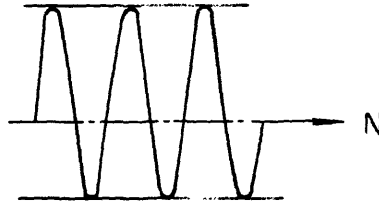
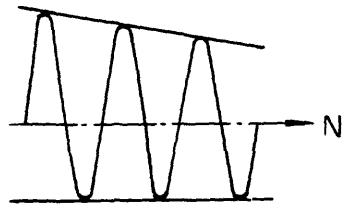
- Fig. 1. Three types of repeated stress cycles.
- Fig. 2. Crack propagation in geometrically similar specimens subjected to repeated stress cycles of constant amplitude. Material: 24S-T;  $2\sigma = 12 \text{ kg/mm}^2$ .
- Fig. 3. Crack propagation in geometrically similar specimens subjected to repeated stress cycles of constant amplitude. Material: 75S-T;  $2\sigma = 12 \text{ kg/mm}^2$ .
- Fig. 4. Effect of initiation period on the transition period.
- Fig. 5. Three  $y + N$  diagrams under various test conditions.
- Fig. 6. Three modes of failure: I tensile; II double shear; III single shear. Arabic numerals indicate number of observed  $(x, N)$  points.
- Fig. 7. Three replicated  $y + N$  diagrams.  $\sigma_0 = 5.49 \text{ kg/mm}^2$ .
- Fig. 8. Three replicated  $y + N$  diagrams.  $\sigma_0 = 2.41 \text{ kg/mm}^2$ .
- Fig. 9. Preceding six diagrams replotted as  $y + N/N_B$  diagrams.
- Fig. 10. Two-level  $y + N$  diagram starting from high stress level.
- Fig. 11. Upper part of diagram in Fig. 10.
- Fig. 12. Two-level  $y + N$  diagram starting from low stress level.
- Fig. 13. Upper part of diagram in Fig. 12.
- Fig. 14. Comparison between schematic two-level  $y + N$  diagrams, one starting from high stress level, the other from low stress level.

LOAD CYCLES

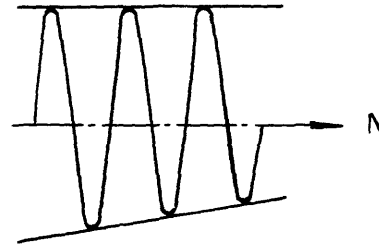
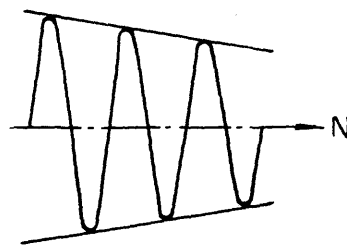
STRESS CYCLES



a) CONSTANT LOAD AMPLITUDE



b) CONSTANT STRESS AMPLITUDE



c) DECREASING LOAD AND STRESS AMPLITUDE

Fig. 1. Three types of repeated stress cycles.



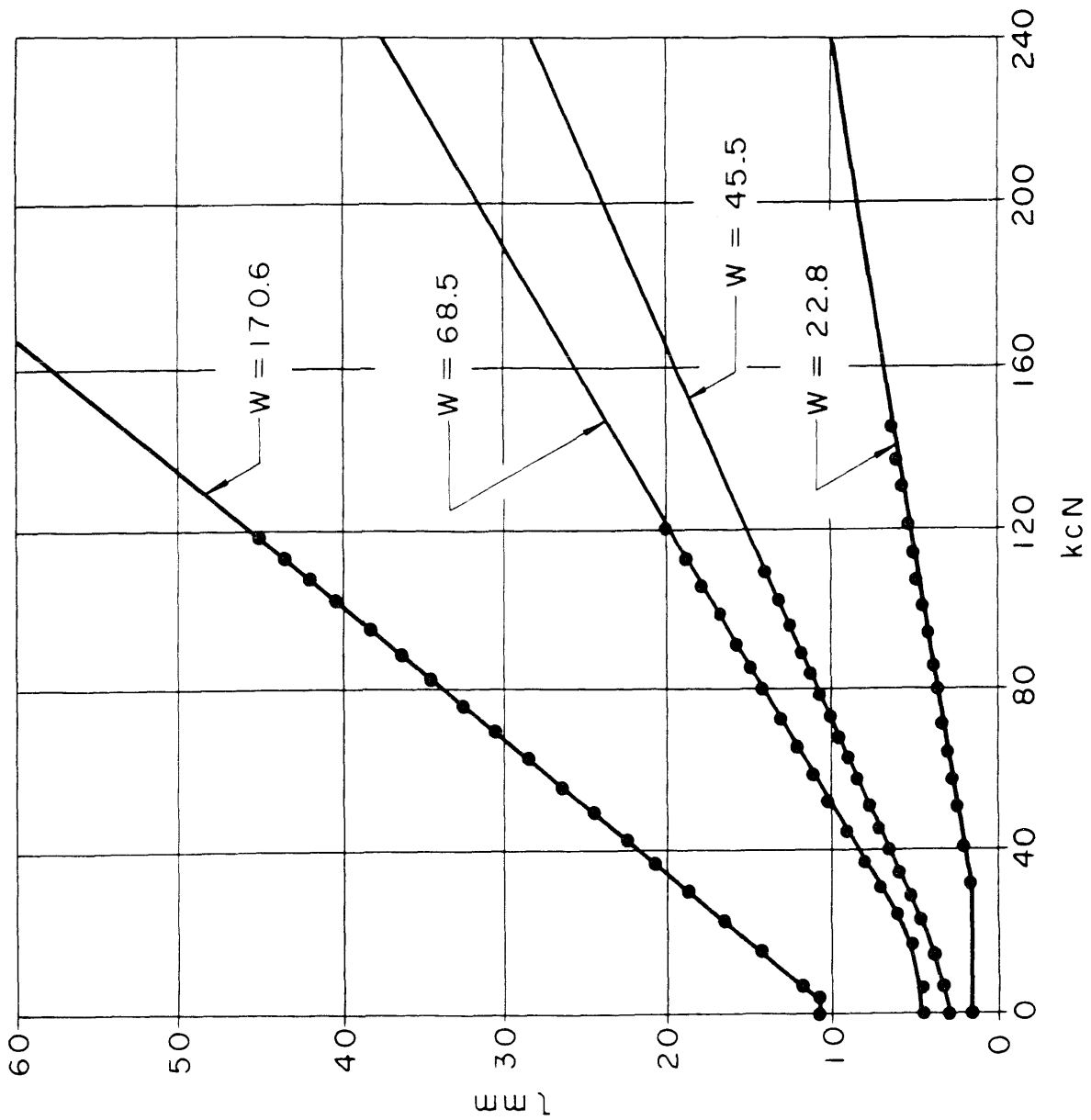


Fig. 2. Crack propagation in geometrically similar specimens subjected to repeated stress cycles of constant amplitude. Material: 24S-T;  $2\sigma = 12 \text{ kg/mm}^2$ .

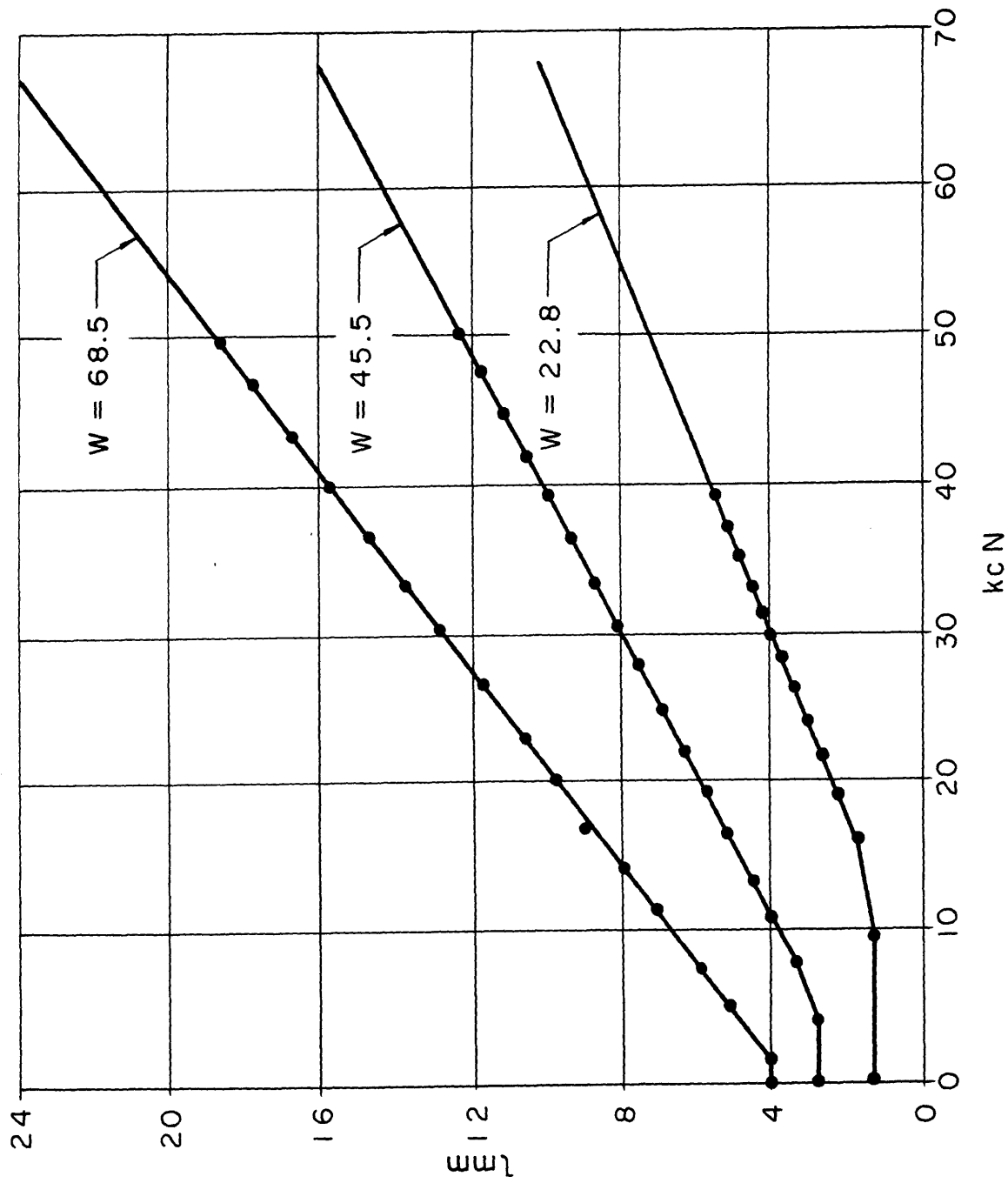


Fig. 3. Crack propagation in geometrically similar specimens subjected to repeated stress cycles of constant amplitude. Material: 75S-T;  $2\sigma = 12 \text{ kg/mm}^2$ .

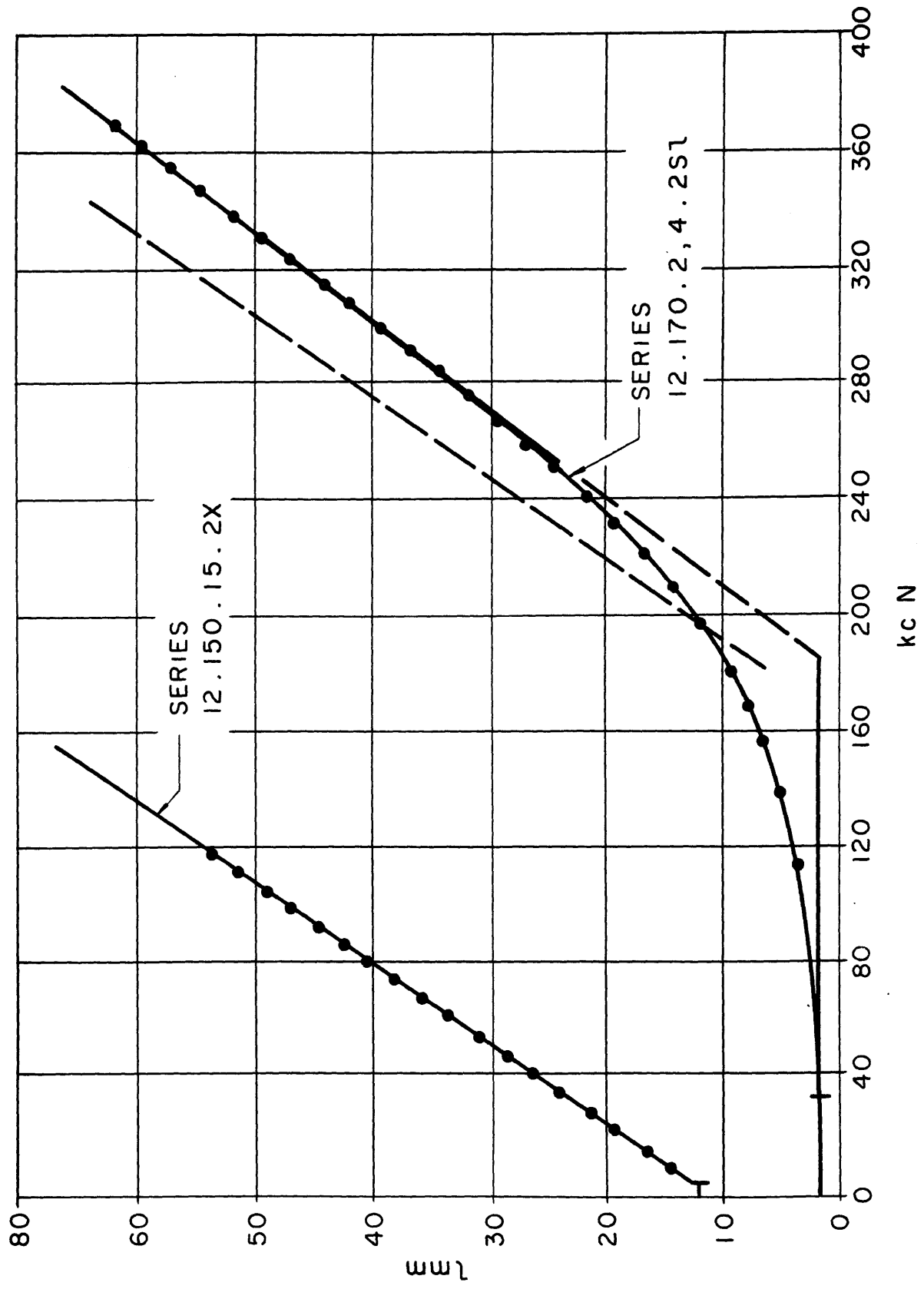


Fig. 4. Effect of initiation period on the transition period.

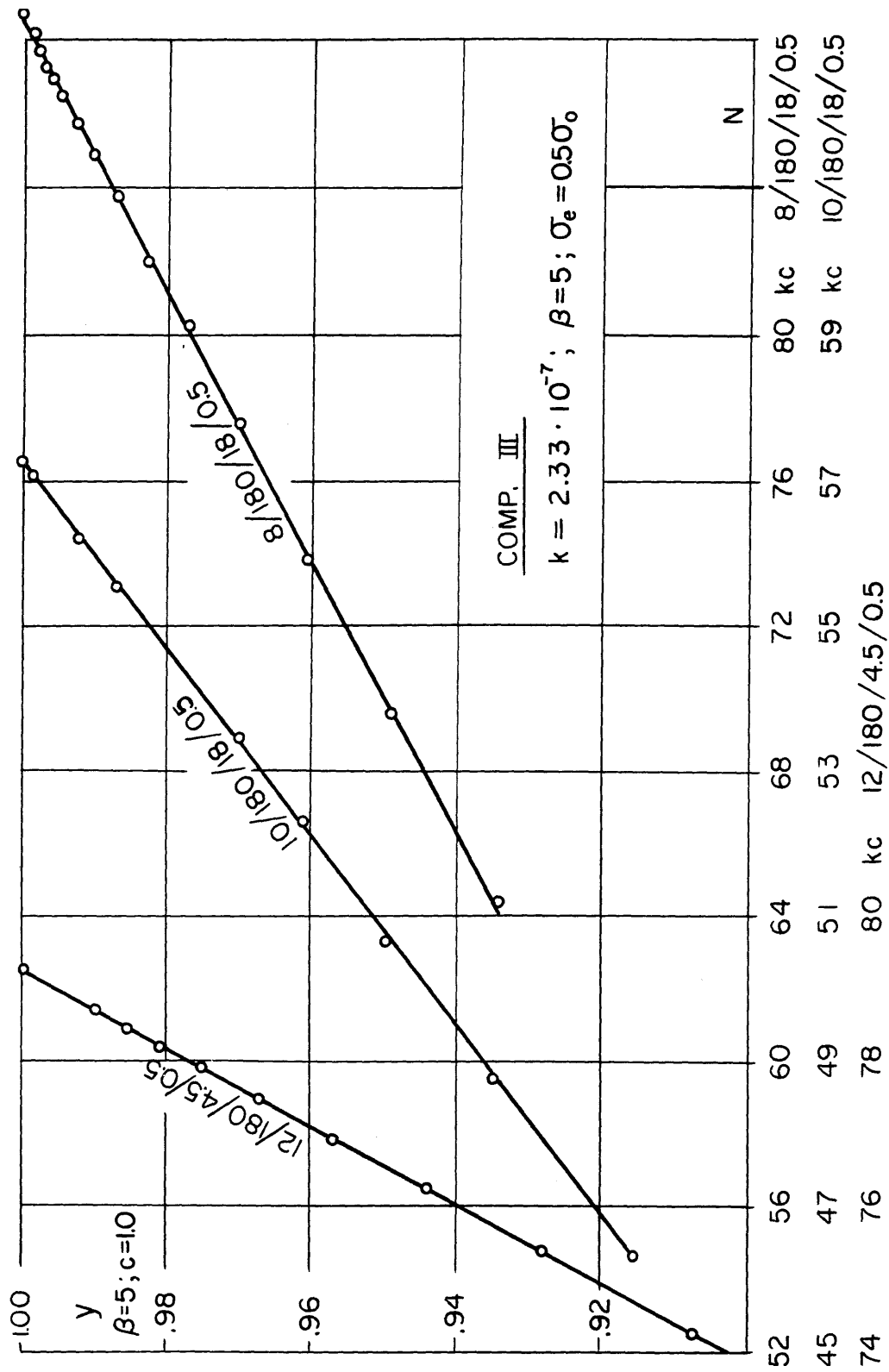


Fig. 5. Three  $y + N$  diagrams under various test conditions.

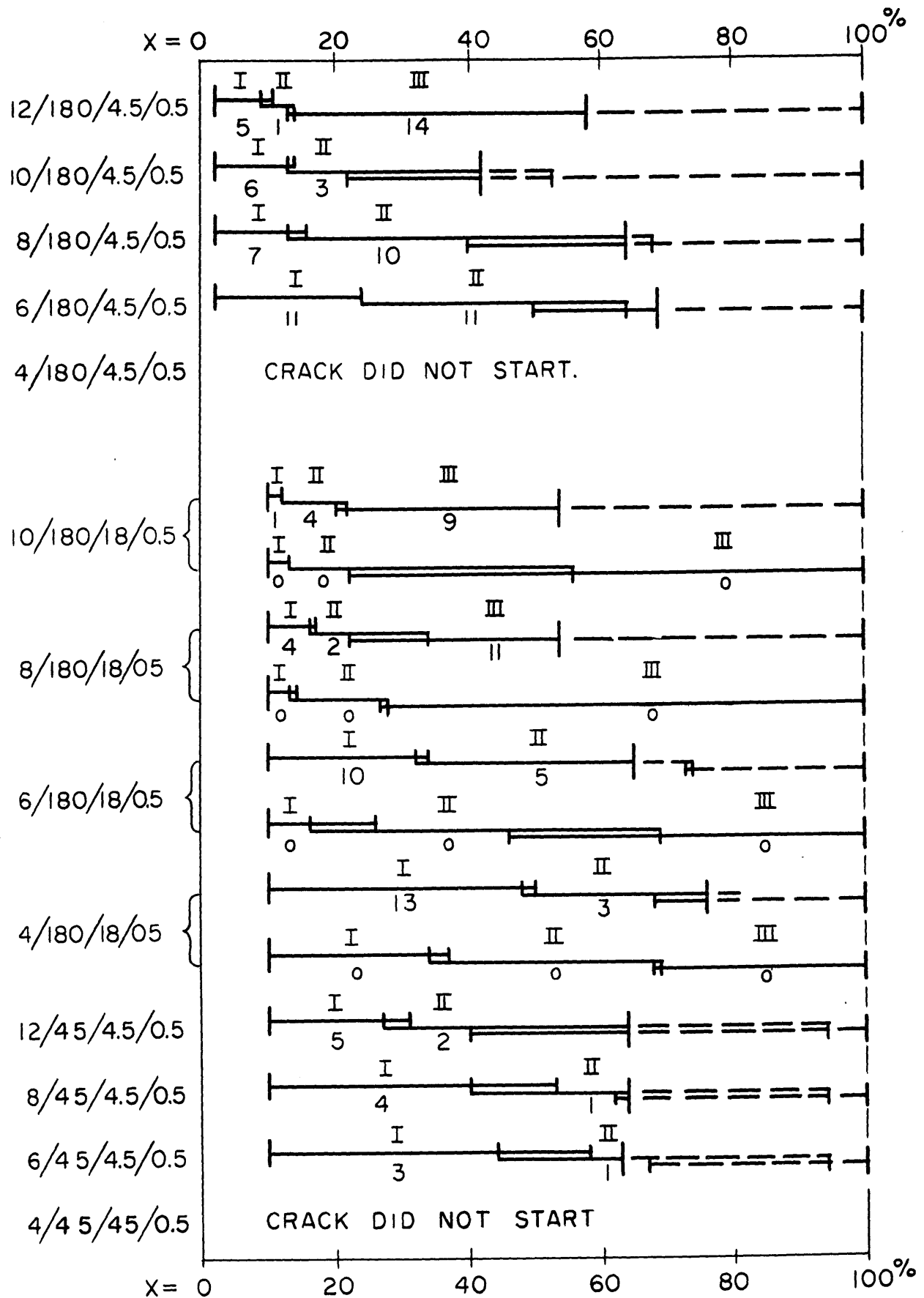


Fig. 6. Three modes of failure: I tensile; II double shear; III single shear. Arabic numerals indicate number of observed (x,N) points.

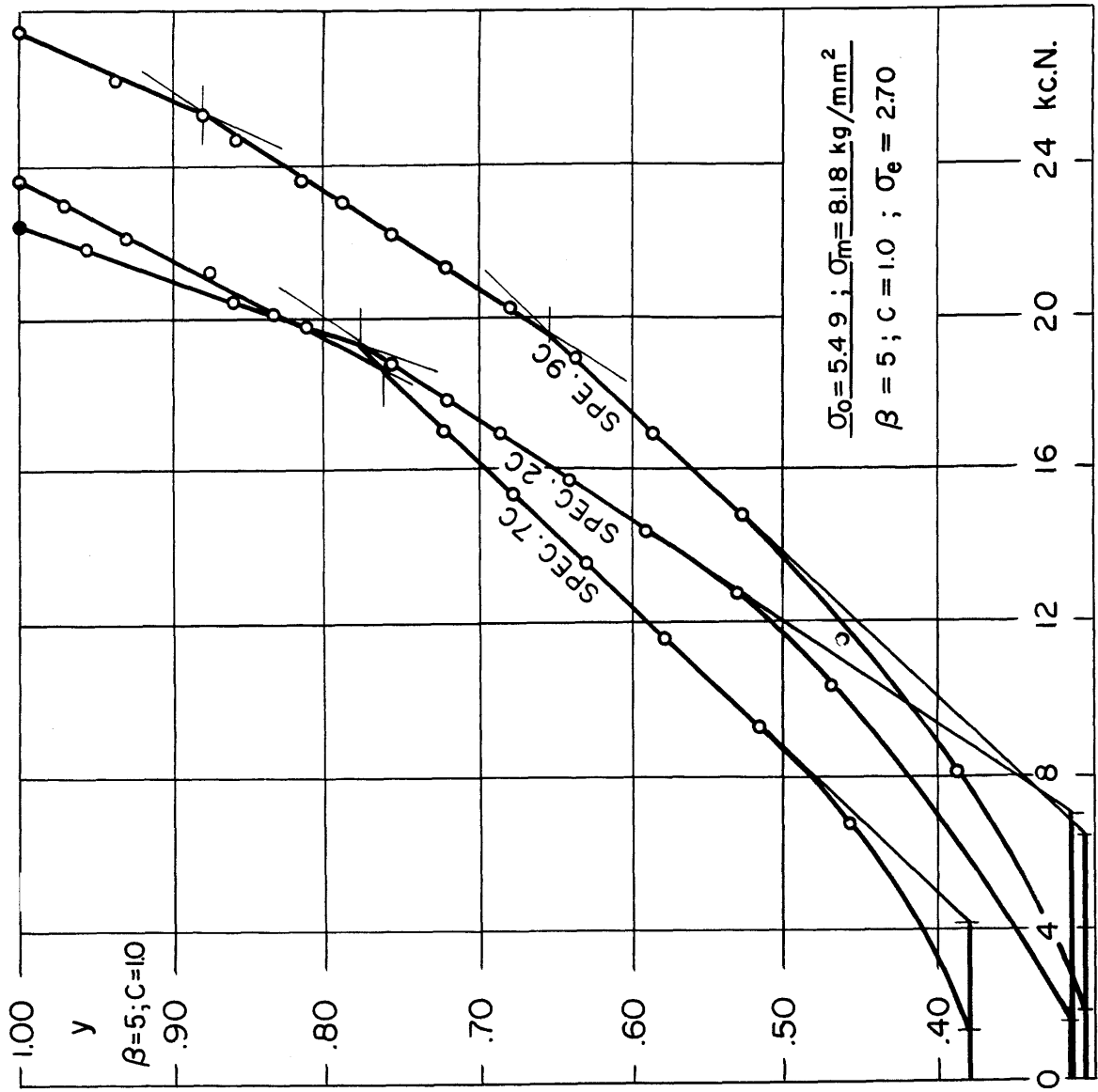


Fig. 7. Three replicated y + N diagrams.  $\sigma_0 = 5.49 \text{ kg/mm}^2$

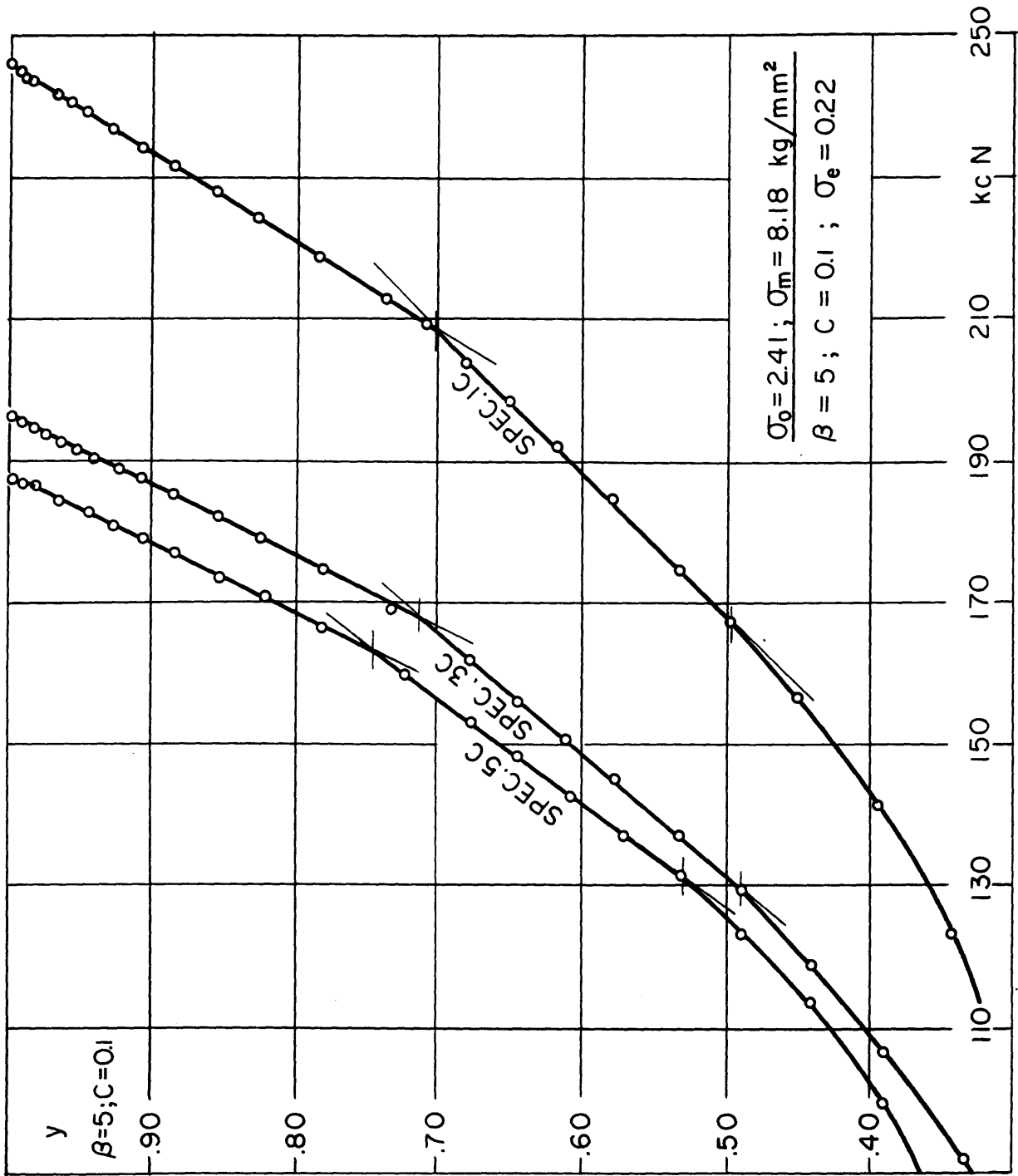


Fig. 8. Three replicated y + N diagrams.  $\sigma_0 = 2.41 \text{ kg/mm}^2$ .

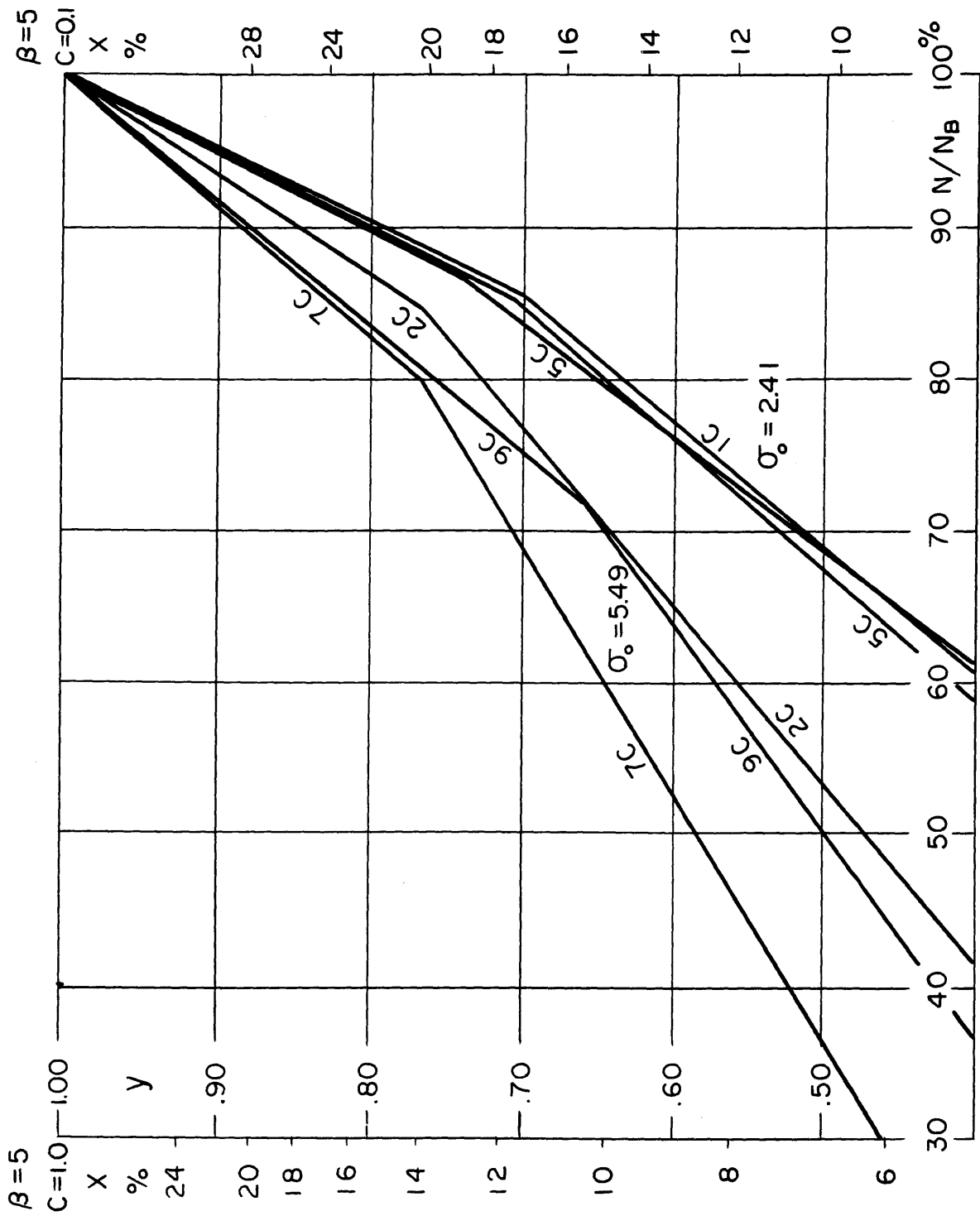


Fig. 9. Preceding six diagrams replotted as  $y + N/N_B$  diagrams.



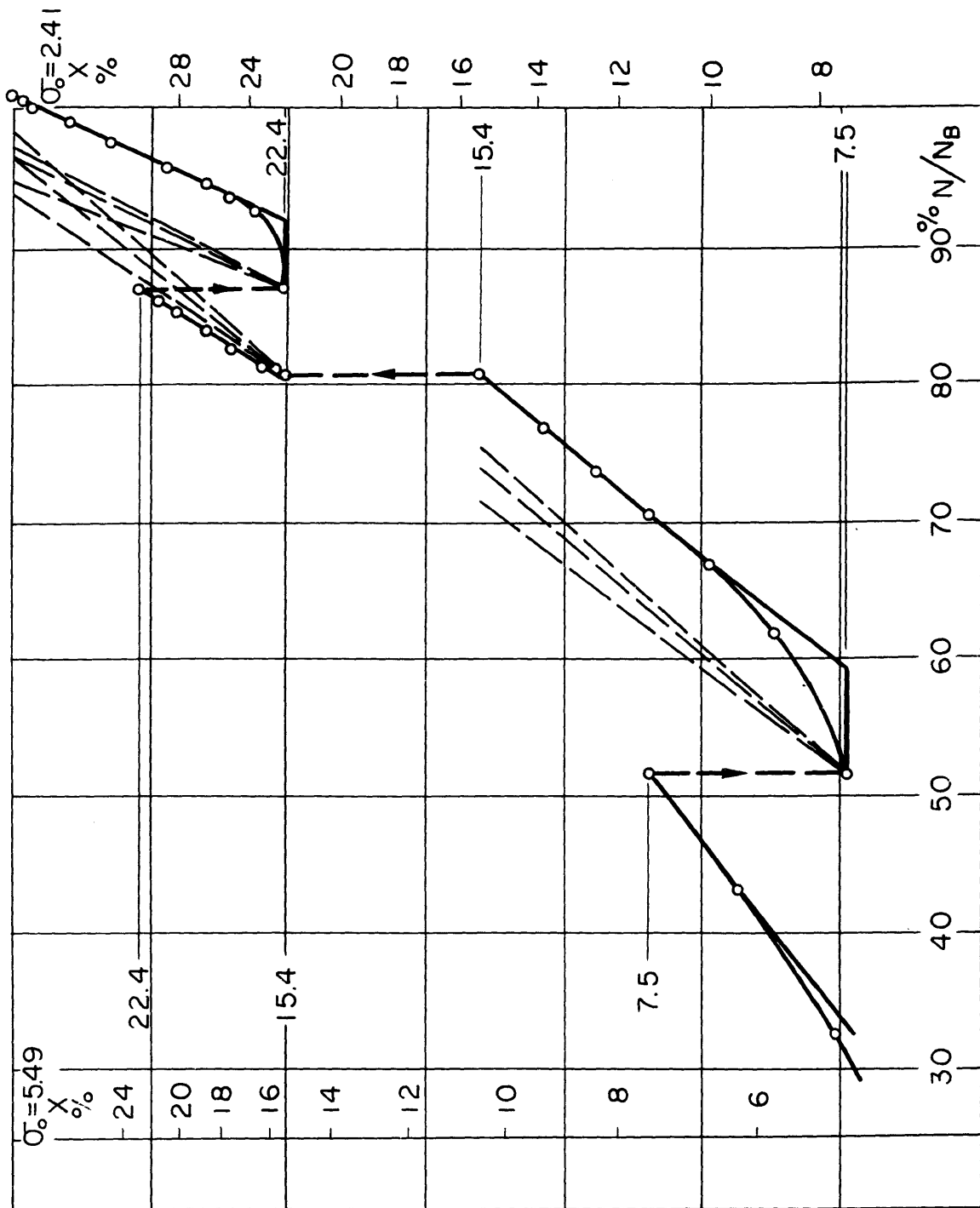


Fig. 10. Two-level y + N diagram starting from high stress level.

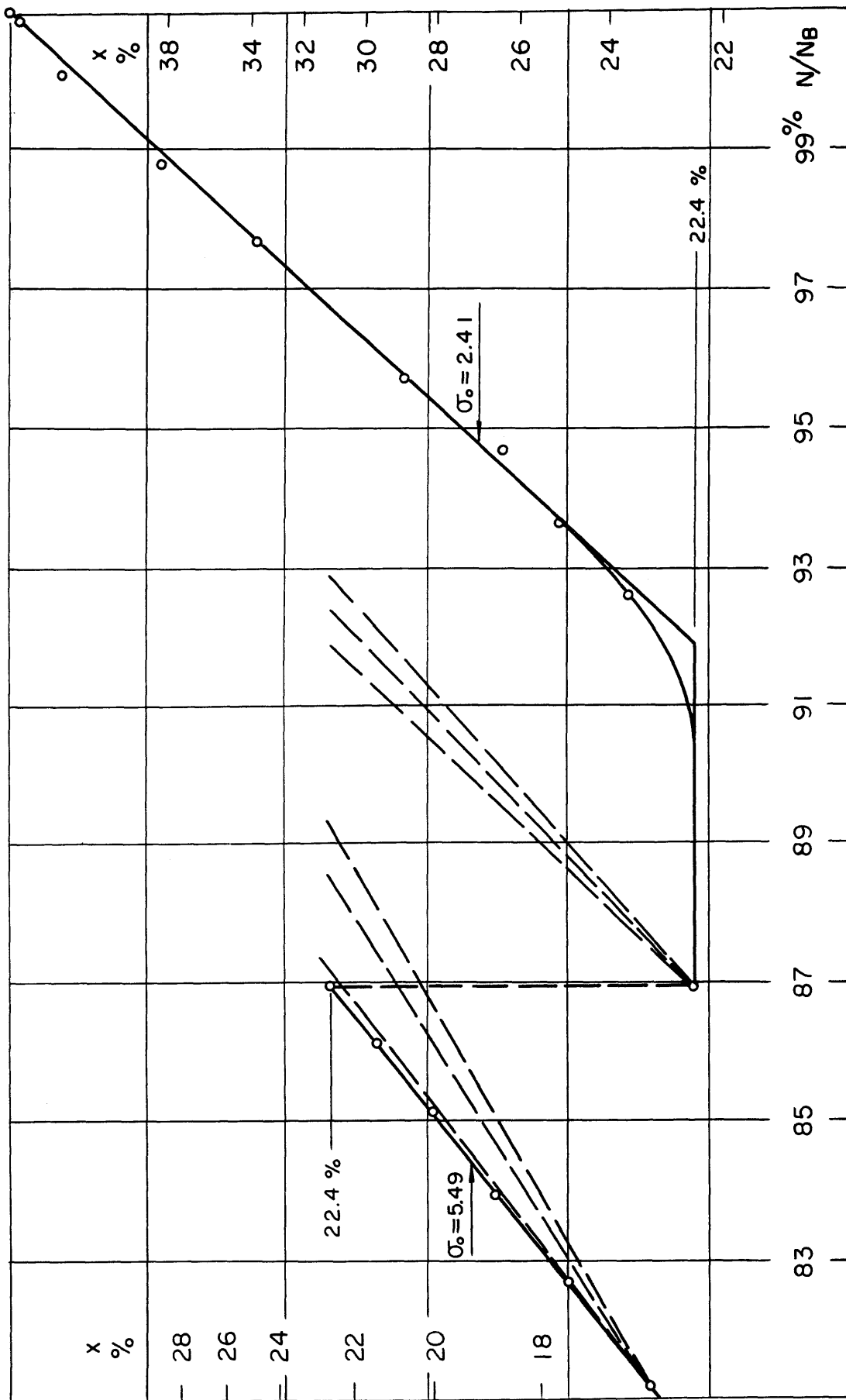


Fig. 11. Upper part of diagram in Figure 10.

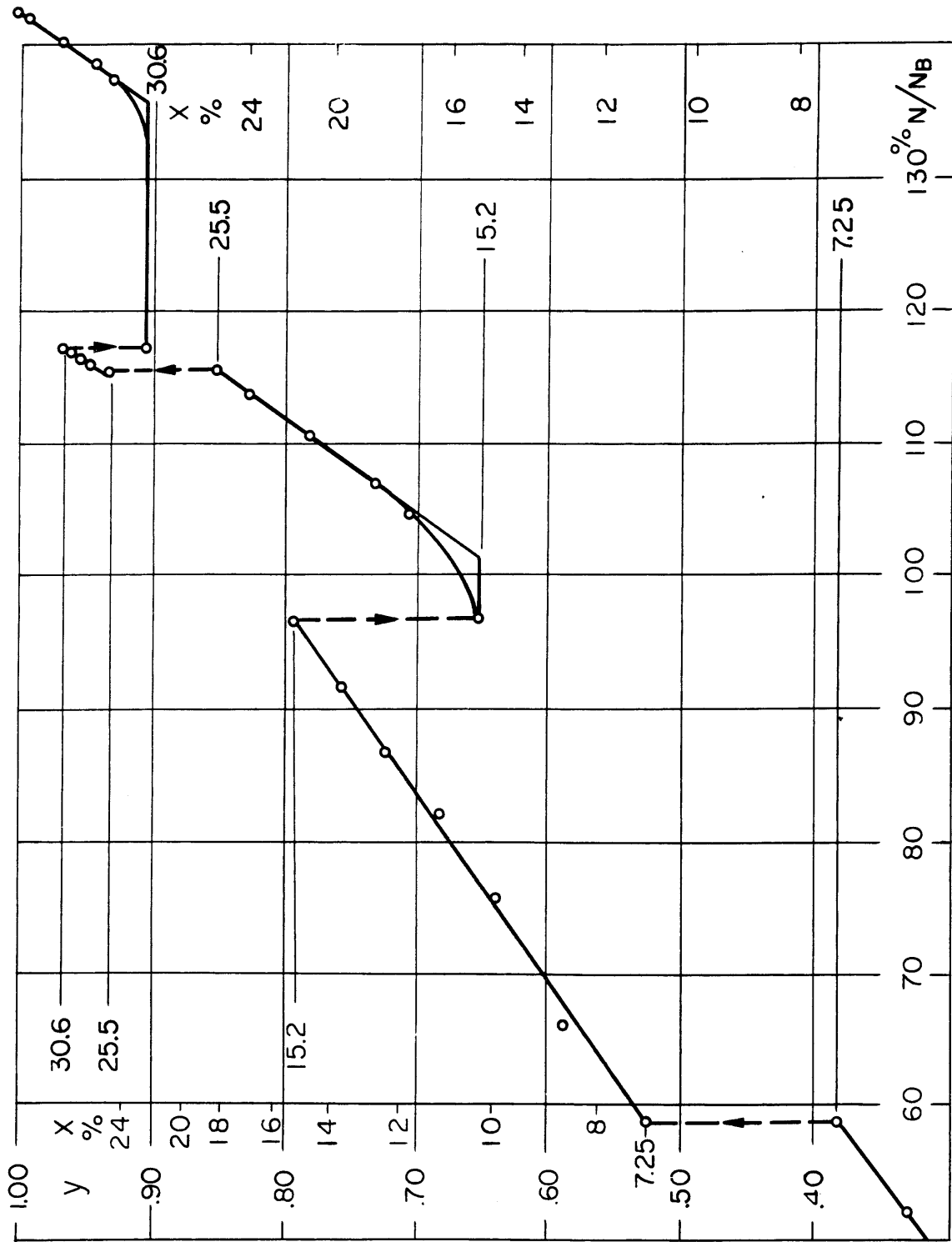


Fig. 12. Two-level y + N diagram starting from low stress level.

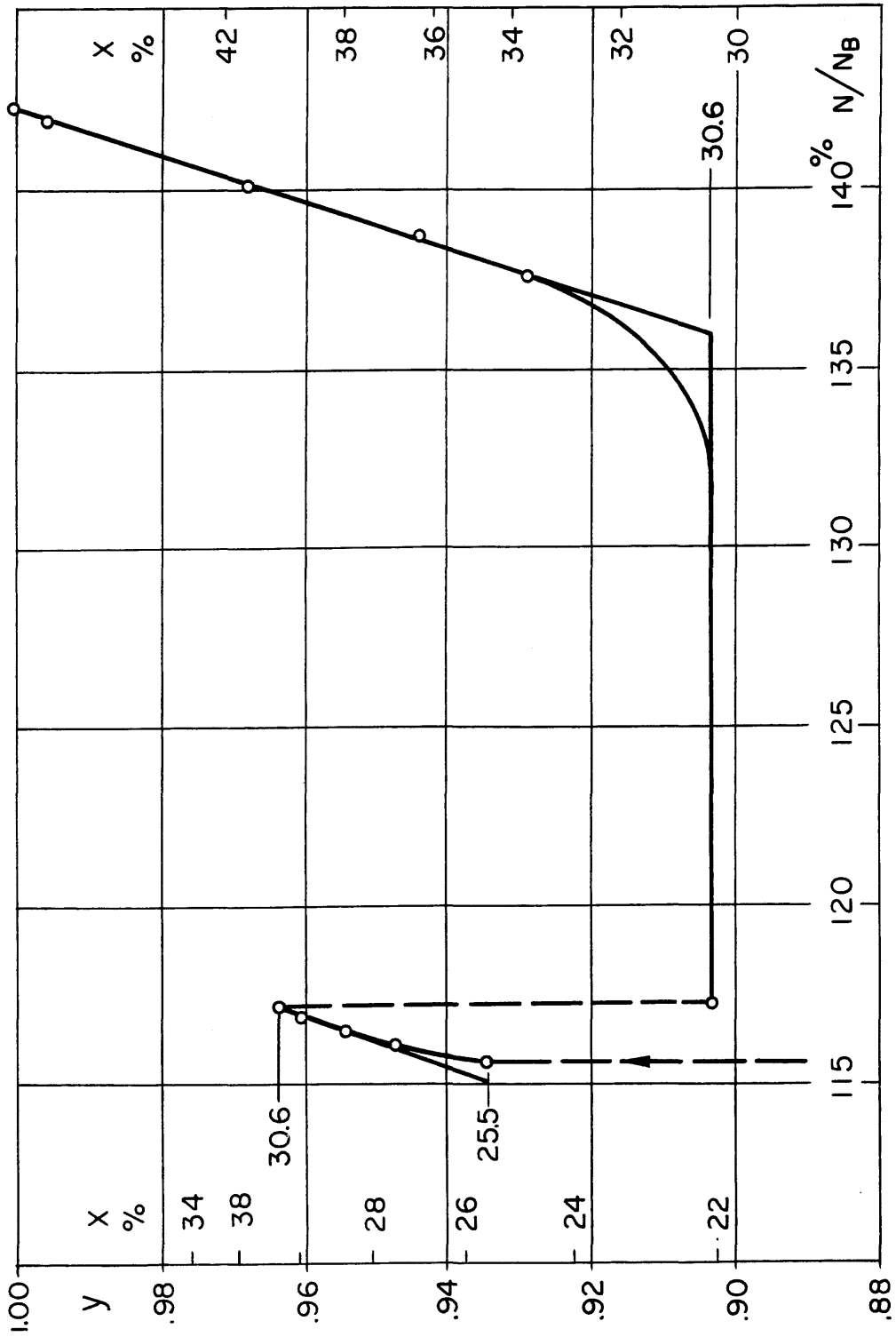


Fig. 13. Upper part of diagram in Figure 12.

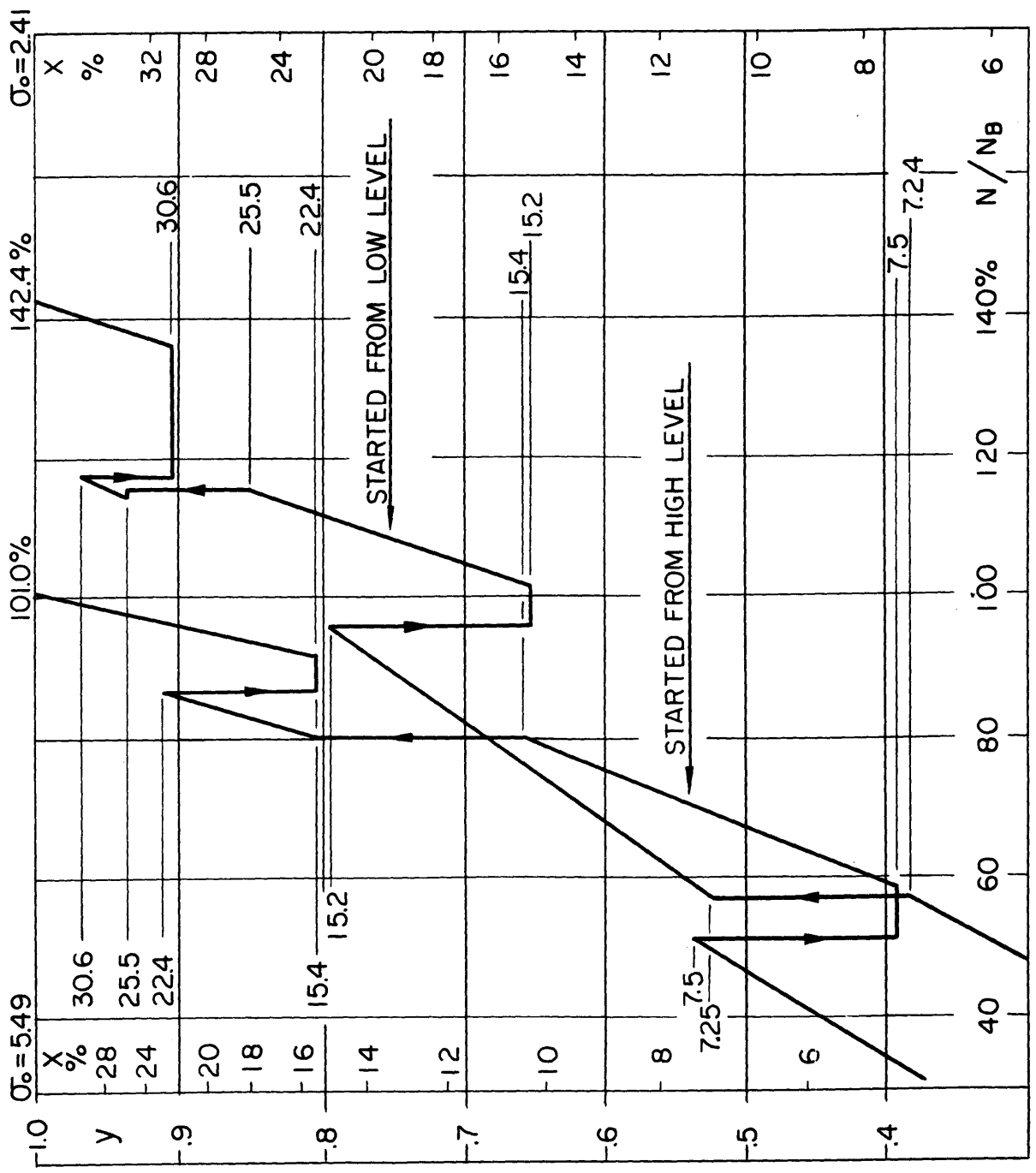


Fig. 14. Comparison between schematic two-level y + N diagrams, one starting from high stress level, the other from low stress level.